

## Flowsheet Design and Modelling for High Purity Praseodymium and Neodymium by Solvent Extraction

<sup>1</sup> Zulkifli N., <sup>1\*</sup> Shoparwe N., <sup>1</sup> Yusoff A.H., <sup>2</sup> Abdullah A.Z., <sup>3</sup> Ahmad M. N.

<sup>1</sup> Gold, Rare Earth and Materials Technopreneurship Centre (GREAT) at Universiti Malaysia Kelantan, Jeli, Malaysia

<sup>2</sup> Universiti Sains Malaysia, Pulau Pinang, Malaysia

<sup>3</sup> Universiti Islam Antarabangsa Malaysia, Kuantan, Pahang, Malaysia

\* Corresponding author email: fazliani.s@umk.edu.my

### ABSTRACT

Purifying rare earth elements (REEs) from ion-adsorbed clay (IAC) deposits demands complex solvent extraction (SX) setups to achieve commercial-grade purity. This study presents the design and validation of a four-train counter-current SX flowsheet for processing a pre-treated REE chloride liquor sourced from Malaysia's Jeli deposit. Using an iterative steady-state mass-balance simulation in Microsoft Excel, the research determines the operational parameters needed to achieve a 4N (99.99%) terminal purity target for each REE stream. The methodology involved pinpointing critical A/B separation cuts and optimising the organic-to-aqueous (O/A) ratios across the cascade. The results show that the flowsheet effectively fractionates the feedstock, starting with a bulk LREE/HREE separation (Train 1) and culminating in the challenging separation of praseodymium (Pr) and neodymium (Nd) (Train 4). The simulation identified Pr/Nd separation as the primary technical bottleneck, requiring 62 equilibrium stages (NE) due to a low separation factor ( $\beta$ ) of 1.70. In contrast, simpler bulk splits needed as few as 16 stages. These findings confirm the theoretical minimum stage requirements ( $N_{min}$ ) and provide a detailed stage-wise concentration profile for each train. The study concludes that the Pr/Nd circuit dictates the overall plant footprint and capital intensity. The developed flowsheet offers a solid technical blueprint for commercialising Malaysian IAC resources, ensuring high-purity REE recovery through optimised metallurgical design.

**Keywords:** REE separation, solvent extraction, P507, equilibrium curve, extraction stages.

### Information about authors:

#### Norazihan Zulkifli

PhD candidate at Gold, Rare Earth and Material Technopreneurship Centre (GREAT), Faculty of Bioengineering and Technology, Universiti Malaysia Kelantan, Jeli 17600 Kelantan, Malaysia. Email: norazihan.zulkifli@gmail.com; ORCID ID: <https://orcid.org/0009-0009-4772-0578>

#### Noor Fazliani Shoparwe

Associate Professor at Gold, Rare Earth and Material Technopreneurship Centre (GREAT), Faculty of Bioengineering and Technology, Universiti Malaysia Kelantan, Jeli 17600 Kelantan, Malaysia. Email: fazliani.s@umk.edu.my; ORCID ID: <https://orcid.org/0000-0002-4329-2459>

#### Abdul Hafidz Yusoff

Associate Professor at Gold, Rare Earth and Material Technopreneurship Centre (GREAT), Faculty of Bioengineering and Technology, Universiti Malaysia Kelantan, Jeli 17600 Kelantan, Malaysia. Email: hafidz.y@umk.edu.my; ORCID ID: <https://orcid.org/0000-0003-0229-886X>

#### Abdullah A.Z.

Professor at School of Chemical Engineering, Engineering Campus, Universiti Sains Malaysia, 14300 Nibong Tebal, Pulau Pinang, Malaysia. Email: chzuhairi@usm.my

#### Mohammad Norazmi Ahmad

Associate Professor at Sustainable Nanotechnology and Computational Chemistry (SuNCoM) Research Group, Department of Chemistry, Kulliyyah of Science, Universiti Islam Antarabangsa Malaysia, 25200 Kuantan, Pahang, Malaysia. Email: mnorazmi@iium.edu.my; ORCID ID: <https://orcid.org/0000-0001-5742-0346>

## Introduction

Rare Earth Elements (REEs), including the 15 lanthanides, scandium, and yttrium, are vital to high-tech sectors such as defense, renewable energy, and electronics [1]. Ensuring a stable and sustainable supply has become a global priority, prompting intensive research into new primary ore sources and innovative recovery methods for secondary materials [[2], [3], [4], [5]]. Robust processing

techniques are essential in the global supply chain for handling complex raw materials such as hydrometallurgical recovery of rare earth elements (REEs) from secondary sources, including neodymium-iron-boron (NdFeB) permanent magnet scrap [6]. Recovering from primary REE sources remains essential, especially as the world shifts its focus to unconventional resources [[7], [8], [9]]. The ion-adsorbed clay (IAC), the raw material for this study, is a complex feed material sourced from the

Jeli deposit in Malaysia. It is an ionic resource extracted by in situ leaching (ISL). This feedstock poses significant challenges owing to its heterogeneity and the complex mixture of light and heavy rare-earth elements (LREEs and HREEs) [10]. Developing a specialised, sophisticated processing method capable of efficiently recovering all valuable REE from ISL liquors, particularly Pr and Nd, is crucial to the successful exploitation of the Jeli resource.

The core technological challenge in the REE industry is the separation of individual elements, which share remarkably similar chemical properties [11]. Historically, solvent extraction (SX) has been the industry standard for commercial-scale, continuous separation [12], with the Lynas Advanced Materials Plant (LAMP) serving as a contemporary benchmark [13]. However, even within world-class facilities, separating the entire REE series presents significant operational hurdles. These challenges highlight gaps in current industrial SX practice, particularly in the number of stages required for the separation of adjacent elements at high purity.

The stringent purity requirements of downstream applications, such as optics and photonics, further complicate process design. For example, the separation of praseodymium (Pr) from neodymium (Nd) is particularly demanding due to its extremely low separation factor ( $b$ ) [14]. Achieving a 99.99% (4N) purity target for these elements is crucial for commercial viability, necessitating complex systems with high stage counts [15]. Research has shown that even trace contaminants can significantly reduce luminescence efficiency in optical materials, as demonstrated by studies comparing Nd, Ho, Er, and Sm oxides in glass matrices [[16], [17], [18], [19], [20], [21], [22]]. Consequently, this application-driven standard mandates that the entire flowsheet reliably produce individual rare-earth oxides at 4N purity.

Ion-exchange (IX) chromatography and crystallisation are typically reserved for laboratory applications or the final purification of high-purity materials. Nevertheless, they are neither scalable nor cost-effective for continuous, large-volume REE separation. For example, even in specific applications such as ion exchange of lanthanum chloride with advanced resins, the process remains inherently batch-oriented, presenting significant scaling challenges compared with continuous SX [23]. The key decision in high-volume REE processing, therefore, lies between IX and SX, as other methods, such as fractional crystallisation, cannot separate the entire REE series [[24], [25],

[26]]. Figure 1 provides a comparative overview illustrating the fundamental differences in mechanism and operation between IX and SX.

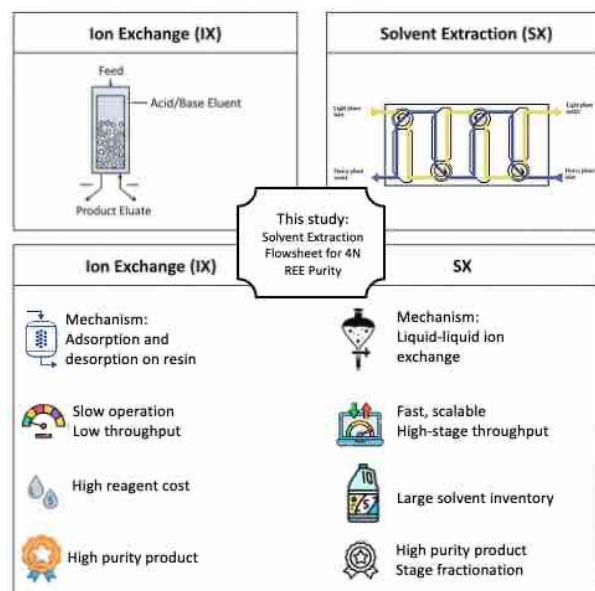


**Figure 1** - Comparative Analysis and Process Principle of Ion Exchange (IX) versus Solvent Extraction (SX) for Rare Earth Element Separation

SX is overwhelmingly preferred for primary industrial separation due to its ability to handle large, continuous throughput. It employs counter-current flow through mixer-settlers or columns relying on subtle differences in distribution coefficients (\$) between adjacent elements. The choice of the organic extractant is the single most critical chemical decision in an SX flowsheet. The acidic extractant bis(2-ethylhexyl) phosphoric acid (P507) was selected for the flowsheet based on its established industrial use and capacity for controllable selectivity via pH adjustments, which is essential for LREE fractionation, particularly the challenging Pr/Nd split [[27], [28]].

Complex mixed-extractant systems are effective for the bulk separation of HREEs; their performance is typically suboptimal for LREE fractionation. For example, the combination of P507 with bis(2,4,4-trimethylpentyl) phosphinic acid (Cyanex 272) [29] or its equivalent, Cyanex 572 [[30], [31], [32]], is known to enhance the extraction of HREEs from chloride solutions. However, in such systems, the resulting enhanced selectivity for HREEs conversely leads to poorer separation performance among the LREE group [33], which constitutes the majority of the Jeli feedstock. Therefore, the use of P507 alone is justified to provide the necessary selectivity

control for the difficult LREE-focused splits required to achieve the 4N purity target.

The highly efficient separation required by SX is achieved physically through a series of interconnected mixer-settler units operating in a counter-current flow configuration, as shown in Figure 2, where Figure 2(a) explains the working principle of a single mixer settler and Figure 2(b) illustrates the separation principle in a series circuit.

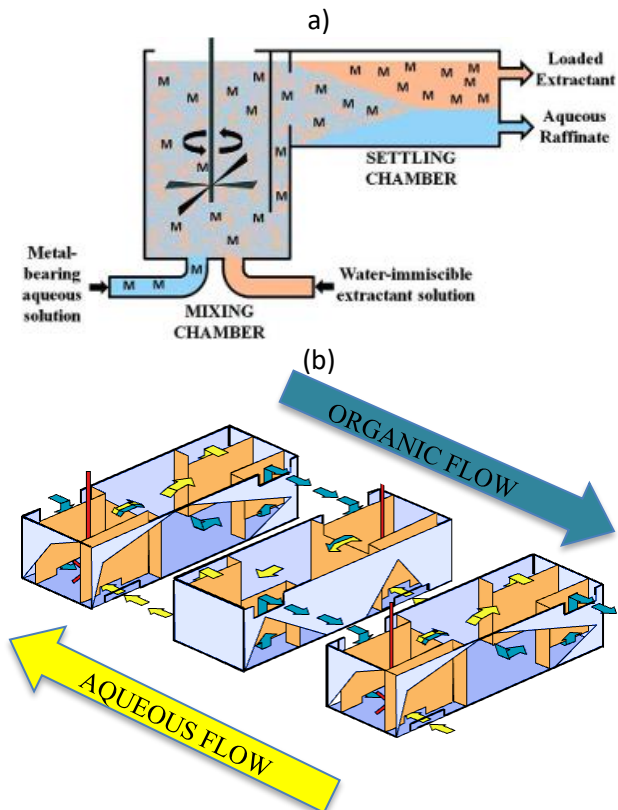


Figure 2 - Working principle of mixer settler

In the mixing chamber, a motor drives a mixing and pumping turbine. This turbine draws two liquids from adjacent settler stages, mixes them and transfers the resulting emulsion to the corresponding settler. Efficient mixing creates a large interfacial area, maximising solute mass transfer. The emulsion then overflows into the settling chamber, where gravity separates the liquids. The heavier aqueous liquid settles at the bottom, while the lighter organic liquid rises to the top and overflows a fixed-height weir. This gravity-driven discharge transports the liquid to the next mixing chamber or downstream equipment.

Rare earth extraction (REEP) is typically a sequential cascade process involving three main stages: extraction, scrubbing, and stripping. Industrial facilities such as LAMP employ a six-stage process comprising saponification, loading,

extraction, scrubbing, stripping, and washing. Figure 3 illustrates this cascade operating under counter-current flow: the organic phase enters at one end, and the aqueous feed enters at an internal stage, moving in the opposite direction.

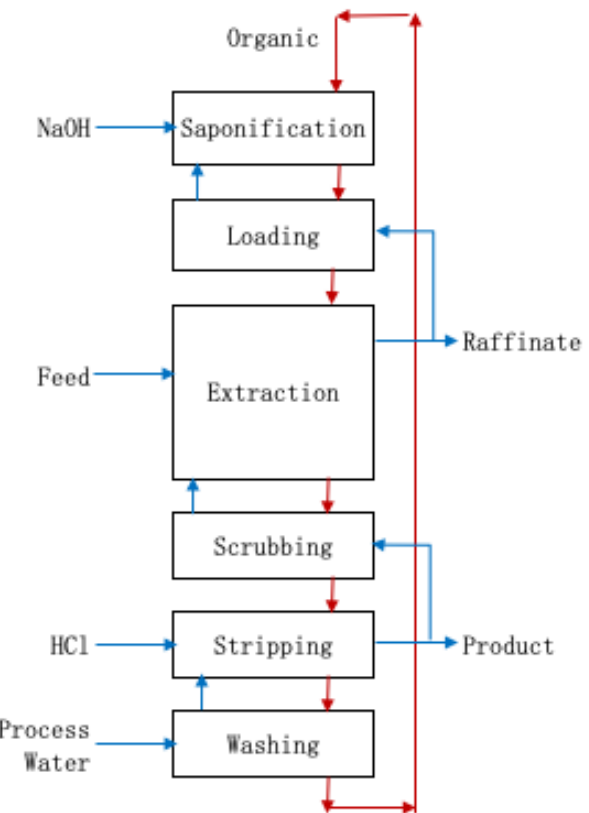


Figure 3 - Schematic Diagram of a Six-Block Counter-Current Solvent Extraction Cascade (Saponification, Loading, Extraction, Scrubbing, Stripping, and Washing).

This inherent counter-current arrangement maximises mass-transfer efficiency, thereby enabling the use of a rigorous mass-balance model. The main challenge in SX design is accurately determining the optimal flow ratios (O/A) and the minimum number of equilibrium stages ( $N_{min}$ ). These parameters are crucial for converting the slight chemical differences provided by P507 into commercial purity.

This study addresses a technological gap by presenting a rigorously designed and validated four-train SX flowsheet for separating a complex mixture of LREE and HREE from the Jeli resource. The primary objective is to rigorously justify the flowsheet's design parameters, particularly the high stage counts required for adjacent-element separation. Using an iterative mass-balance model, the paper systematically derives the overall-to-actual flow ratios. It calculates the necessary

equilibrium stages ( $N_E$ ) to ensure the flowsheet can produce individual rare-earth oxide products to the stringent 4N purity standard.

## Experimental part

**Materials and Feedstock Preparation.** The feed material for the SX flowsheet design was a pre-treated REE chloride solution from the Jeli deposit in Malaysia. The original Jeli IAC resource was initially processed via the ISL hydrometallurgical route to produce a bulk REE liquor. To ensure high-purity separation, the liquor underwent upstream purification, including selective precipitation and redissolution, to concentrate REEs and remove non-metallic contaminants and gross impurities such as silica and carbonates. The resulting clarified REE chloride solution was the primary input for iterative mass-balance modelling. The elemental composition is detailed in Table 1, with concentrations expressed in both parts per million (ppm) and as a mass percentage of the total REE content.

**Theoretical Framework of Solvent Extraction.** The SX process using P507 operates via an ion-exchange mechanism. In the organic phase, P507 (usually represented as HL) predominantly exists as a dimer ( $HL_2$ ). During extraction, the trivalent REE ion ( $REE^{3+}$ ) from the aqueous phase replaces the protons ( $H^+$ ) in the extractant dimer, forming an organometallic complex that then partitions into the organic phase. The balanced chemical equation for this extraction is given by Equation 1.



In practice, the extraction complex can be solvated and the number of extractant molecules per metal ion may vary. The distribution coefficient ( $D$ ) is strongly inversely related to aqueous pH (or  $H^+$  concentration) as shown in the equilibrium relationship of Equation 2.

$$D = \frac{[REE]_{org}}{[REE]_{aq}} = K_{ex} \frac{[(HL)_2]_{org}^3}{[H^+]_{aq}^3} \quad (2)$$

This relationship demonstrates that aqueous-phase acidity and extractant concentration govern the extent of extraction. These dynamics are typically visualised through extraction isotherms, which illustrate how pH adjustments are leveraged to control extraction and stripping across the various flowsheet trains [34].

**Table 1** - Jeli mix REE chloride composition

Element	Concentration (ppm)	Normalised Concentration (%)
REE		
La	1245.431	38%
Ce	161.159	5%
Pr	211.278	6%
Nd	596.106	18%
Sm	88.268	3%
Eu	11.463	0%
Gd	115.513	4%
Tb	18.351	1%
Dy	94.645	3%
Ho	17.166	1%
Er	83.993	3%
Tm	12.583	0%
Yb	52.871	2%
Lu	5.359	0%
Y	578.472	18%
Sc	0.104	0%
Total	3292.762	100%
Non-REE		
Al	0.950	-
Pb	0.381	-
Cu	0.259	-
Ga	0.227	-
Ca	0.141	-
Al	0.056	-
Pb	0.048	-
Na	0.047	-
Mo	0.040	-
Sr	0.017	-
Co	0.015	-
Ag	0.005	-
Mg	0.001	-
Total	2.187	-

The required  $N_E$  for a counter-current SX circuit is fundamentally governed by  $\beta$  of the critical adjacent pair and the stringency of the purity requirement.  $\beta$  is defined as the ratio of D of the two elements being separated (A and B), where  $\beta$  is the most extracted element, and A is the least attracted component. This is expressed in Equation 3.

$$\beta_{B/A} = \frac{D_B}{D_A} \quad (3)$$

The theoretical  $\beta$  values used were sourced from the literature, primarily the work of Krishnamurthy Gupta (1990) [35] for the P507-HCl REE extraction system [36]. A high  $\beta$  facilitates an efficient separation, whereas a low  $\beta$  necessitates an increased number of mixer-settler contacts to achieve the same purity [37].  $N_{min}$ , is approximated using the relationship derived from the Fenske equation, as shown in Equation 4.

$$N_{min} = \frac{\log\left(\frac{\text{Purity Ratio}}{\text{Recovery Ratio}}\right)}{\log(\beta)} \quad (4)$$

In this context, the purity ratio is the ratio of the key component B to the impurity A in the final product stream. The recovery ratio is the ratio of B recovered in the product stream to the amount of A lost to the raffinate.

This requirement justifies the complex design and detailed mass-balance analysis in the following sections.

**Flowsheet Design and Mass Balance Methodology.** The practical number of equilibrium stages ( $N_E$ ) and the required organic-to-aqueous ratio (O/A; R) were determined using a process simulation developed in Microsoft Excel. The schematic representation of the counter-current mixer-settler stage configuration used as the basis for this mass-balance calculation is presented in Figure 4.

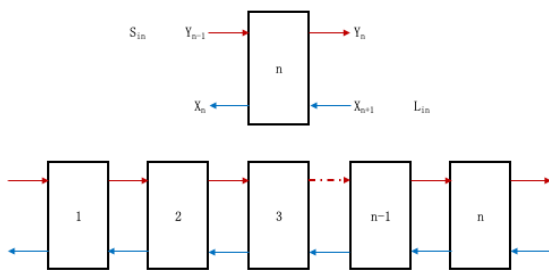


**Figure 4** - Input and output flow variables for a mixer-settler stage configuration

This iterative approach is essential for accurately modelling the complex requirements of ultra-high-purity targets (4N), where conventional graphical methods often lack the precision required to resolve concentrations at the 0.01% threshold. The 4N target purity necessitates a high stage count throughout the flowsheet. To achieve this, the impurity concentration in each product stream must

be rigorously reduced, thereby approaching near-total theoretical recovery in the respective raffinate and extractant streams. This design philosophy is most critical for separating the Pr/Nd pair, the most capital-intensive step in the process.

The initialisation of the solvent flow was based on a fractional extraction approach. A base flow parameter ( $W$ ) was established as a function of  $\beta$  and a fractional extraction parameter ( $K$ ).

$$W = \frac{1}{\beta^{K-1}} \quad (5)$$

For the Jeli flowsheet,  $K$  was optimized at 0.75. This value was selected to bias the extraction intensity toward the organic phase, thereby shifting the concentration crossover point toward the extract terminal. This design strategy aims to provide an expanded scrubbing section within the calculated cascade, ensuring that the aqueous raffinate meets 4N requirements by effectively "washing" entrained impurities from the organic phase. To account for the mass flux required to satisfy terminal purity targets ( $P$ ) and feed fractions ( $f$ ), the final Total Organic-to-Aqueous Ratio ( $R$ ) was calculated as equation 6.

$$R = W + \left( \frac{f_A P_B}{P_A} \right) \quad (6)$$

A key feature of this flowsheet design is the requirement for 4N purity in intermediate product fractions. While a lower intermediate target (e.g., 2N or 3N) would reduce the stage requirements of the preceding separation cascades, it would introduce an "impurity carryover" effect. By enforcing a 4N target at these intermediate steps, the flowsheet acts as a metallurgical firewall, ensuring that downstream circuits are not burdened with residual light or heavy impurities from prior splits. This isolation prevents a "snowball effect," in which downstream-stage requirements would otherwise increase significantly to accommodate cross-contamination. This strategic approach ensures that each separation battery operates only on its intended adjacent pairs, maintaining the integrity of the final high-purity oxides.

After defining the cut, the simulation iteratively calculated concentration profiles across all stages until terminal concentration requirements were satisfied. At stage  $n$ , the total mass balance for component A is given by Equation 5, where  $L$  and  $S$  represent the aqueous and organic flow rates, respectively.

$$(L \cdot X_{n-1}) + (S \cdot Y_{n+1}) = (L \cdot X_n) + (S \cdot Y_n) \quad (5)$$

By substituting  $D_A$  with  $Y_n/X_n$  and the flow ratio A/O as represented with  $R$  equivalent to  $S/L$ , the balance solved in the iterative form shown in Equation 6.

$$X_{n-1} + R \cdot D_A \cdot X_{n+1} = (L + R \cdot D_A) \cdot X_n \quad (6)$$

This modelling relies on the assumption of ideal equilibrium behaviour at each stage and constant flow rates throughout the cascade. The simulation explicitly examines the separation of adjacent elements within each train, aiming for near-total recovery driven by strict 4N terminal purity requirements. Table 2 outlines the key inputs for the iterative mass-balance model, including the derived  $\beta$  and the resulting  $N_{min}$  needed to achieve the 4N purity target for each critical separation train.

## Results and Discussion

The complex composition of the Jeli feedstock necessitates a sequential, four-train SX flowsheet to achieve the stringent 4N purity target for rare-earth oxides. This flowsheet prioritises broader bulk splits before addressing more chemically similar cuts, exploiting differences in  $\beta$  values between adjacent elements. The Pr/Nd separation primarily dictates the overall flowsheet scale and capital intensity, as its low  $\beta$  of 1.70 necessitates the highest number of stages. After calculating  $N_{min}$ , an iterative mass-balance simulation was used to determine the necessary operational parameters, specifically the optimal O/A ratio and the  $N_E$  required to achieve the 4N purity target for each split. Figure 5 presents the block diagram for the four-train sequential SX flowsheet, summarising the proposed processing route. It details the mass distribution and specific fractional cuts for the Jeli REE chloride feedstock, progressing from the initial bulk LREE/HREE split to the final high-purity products.

**Table 2** – Summary of  $\beta$ , target purities, and  $N_{min}$  for the Jeli REE separation aims

Train	Separation Cut	$\beta$	Component		Fraction In Feed		Target Purity		$K$
			A	B	$f_A$	B	$P_A$	$P_B$	
1	LaCePrNd/Sm-Lu	8	LaCePrNd	Sm-Lu	0.65	0.35	99.99%	99.99%	0.75
2	LaCe/PrNd	2.25	LaCe	PrNd	0.64	0.36	99.99%	99.99%	0.75
3	La/Ce	6	La	Ce	0.88	0.12	99.99%	99.99%	0.75
4	Pr/Nd	1.70	Nd	Pr	0.25	0.75	99.99%	99.99%	0.75

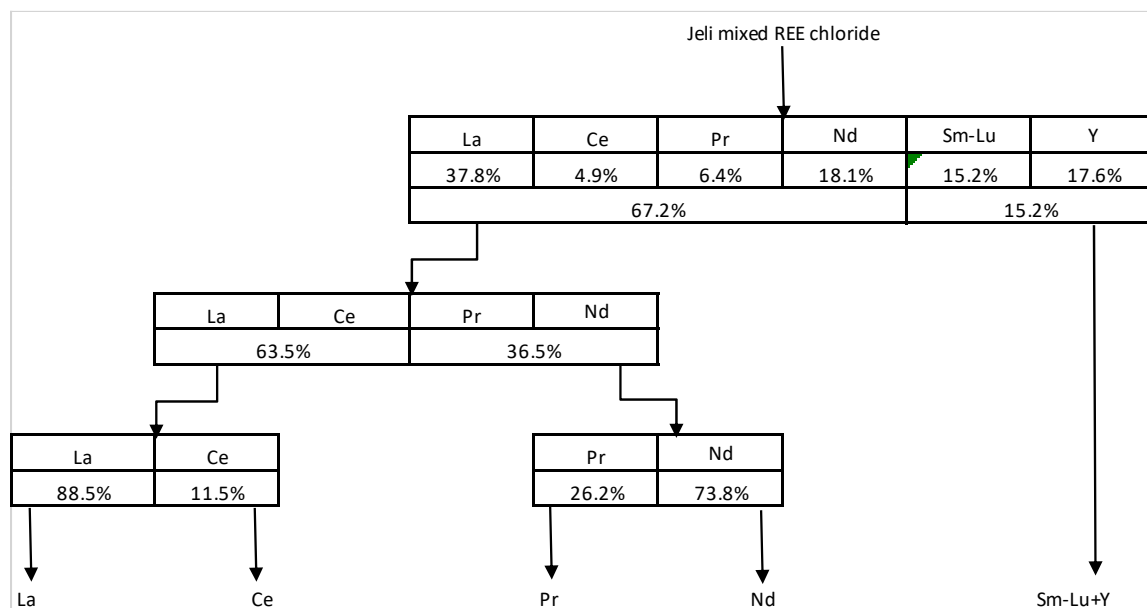


**Figure 5** - Block diagram of the proposed four-train sequential solvent extraction flowsheet for Jeli REE chloride feedstock

Figure 6 illustrates the concentration profiles of components A and B across the extraction stages. Stage 1 (leftmost terminal) is the raffinate outlet, highly enriched in the least-extracted element (A). Stage 2 (rightmost terminal) is the extract outlet, enriched in the most-extracted element (B). The crossover point, where A and B concentrations intersect, shifts with different separation factors. Figure 6 (a) (LREE/HREE,  $\beta = 8.0$ ) shows a sharp crossover, indicating efficient separation with fewer stages. Figure 6 (d) (Pr/Nd,  $\beta = 1.70$ ) shows a shallower gradient, indicating greater difficulty in separation and requiring more stages to reduce impurity levels to 0.01%. Figure 7 presents the separation flowsheet matching the stage numbers for each train.

The final operational deliverables, determined by the iterative mass-balance model, are shown in Table 3. The data confirm that the 4N purity target for both the raffinate (PA) and extract (PB) streams was achieved in all four separation trains. A comparison between  $N_{min}$  and  $N_E$  reveals a consistent scaling factor of 1.8. Table 3 also compares the total stage count required for each train, highlighting the disparity in separation difficulty. Notably, Train 4 (Pr/Nd) requires the most intensive configuration, with an  $N_E$  of 62 stages to overcome the pair's low separation factor. This is nearly four times the stage count required for the bulk LREE/HREE split (Train 1), highlighting the significant impact of adjacent-element chemistry on total plant footprint.

The findings confirm the industrial principle that the Pr/Nd separation is the main bottleneck, limiting the maximum CAPEX and OPEX of the entire LREE purification facility. The 62-stage cascade requires a large physical footprint and complex process control for flow rates and pH stability. However, the simulation shows that the optimised O/A ratios in Table 3 can reliably achieve high recovery and purity without significant material loss.

## Conclusions

This study developed and validated a four-train counter-current solvent extraction flowsheet for processing a pre-treated REE chloride solution from the Jeli IAC deposit. An iterative steady-state mass-balance simulation determined operational parameters for a stringent 4N purity target for five product streams.

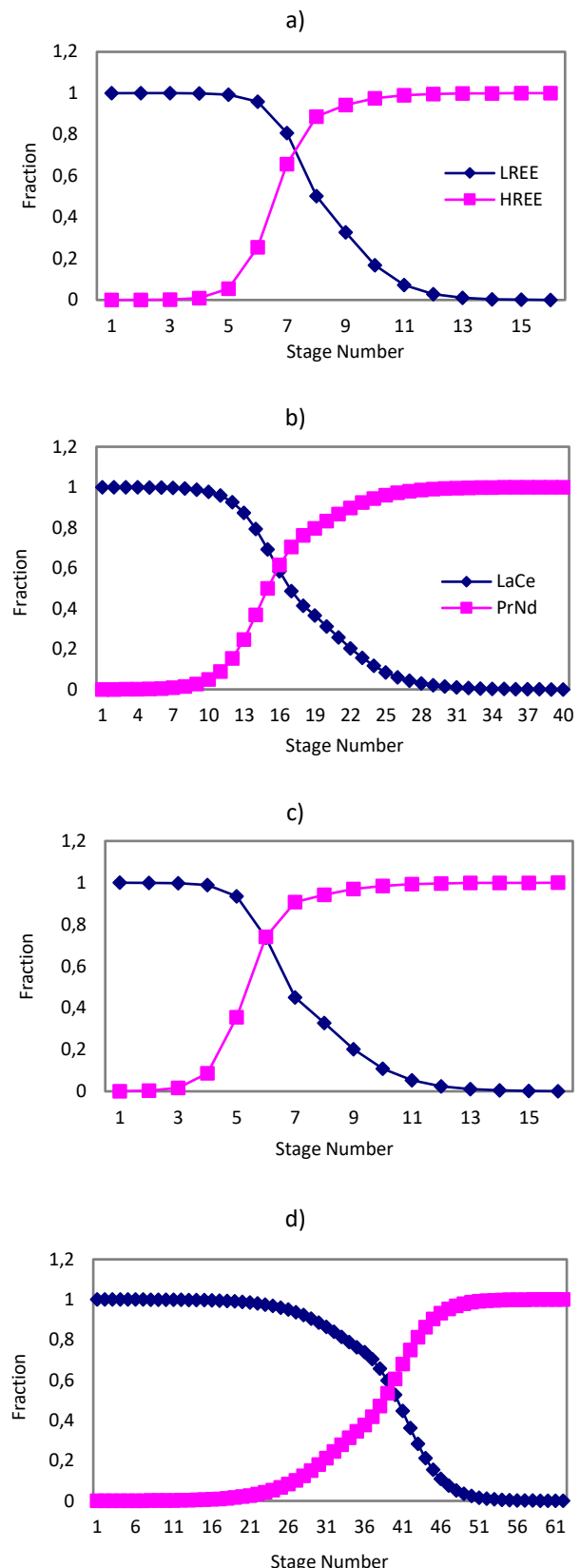


**Figure 6 – Extraction battery concentration profile**  
a) LREE/HREE (67:15,  $\beta=8$ ), b) LaCe/PrNd (64:36,  $\beta=4.57$ ),  
c) La/Ce (88:12,  $\beta=6$ ), and Pr/Nd (76:24,  $\beta=1.7$ )

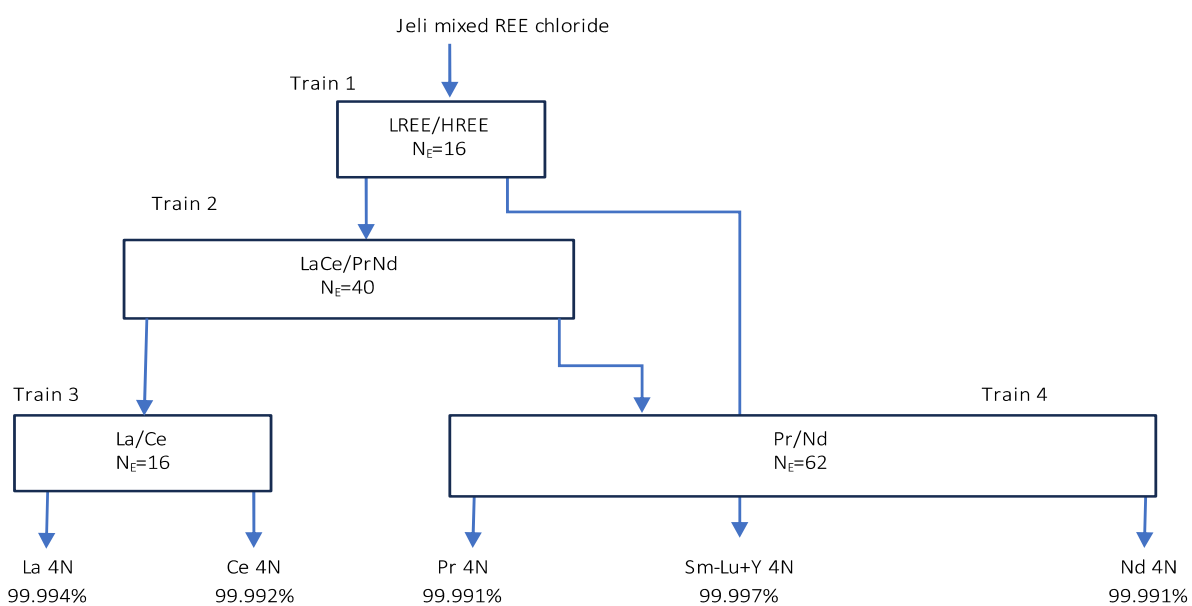


Figure 6 – LREE separation process flowsheet with P507-HCl

Table 3 – Input to equilibrium state calculation

Train	Separation Split (A/B)	Theoretical Minimum Stages (N <sub>min</sub> )	Actual Equilibrium Stages (N <sub>E</sub> )	Optimized O/A Ratio	Purity A (P <sub>A</sub> )	Purity B (P <sub>B</sub> )
1	LaCePrNd/Sm-Lu	8.86	16	0.27	99.99%	99.99%
2	LaCe/PrNd	22.72	40	1.20	99.99%	99.99%
3	La/Ce	10.28	16	0.35	99.99%	99.99%
4	Pr/Nd	34.72	62	2.32	99.99%	99.99%

The Pr/Nd separation (Train 4) is the critical design bottleneck due to its low separation factor ( $\beta = 1.70$ ), requiring 62 equilibrium stages, a nearly four-fold increase compared to the 16 stages required for initial LREE/HREE bulk split.

This high stage count affects the primary capital expenditure (CAPEX) and operational complexity (OPEX), requiring precise control over O/A ratios and pH stability to prevent material loss. Simulation results in Table 3 show that  $N_E$  aligns with  $N_{min}$ , providing a foundation for future pilot-scale testing. The successful separation of La, Ce, and the PrNd group from the Jeli feedstock demonstrates the technical feasibility of producing high-value individual rare earth oxides from Malaysian ion-adsorbed clay resources. This flowchart offers a scalable plan for processing IAC ores, which helps

create a local and sustainable rare earth supply chain.

**Conflicts of interest.** On behalf of all authors, the corresponding author states that there is no conflict of interest.

**Credit author statement:** N. Zulkifli: Conceptualization, Methodology; N. Shoparwe: Supervision; A. H. Yusoff: Co-supervision; A. Z. Abdullah: Co-supervision; M. N. Ahmad: Co-supervision.

**Acknowledgements.** This work was supported by the GREAT Universiti Malaysia Kelantan Research Fund grant number R/FRGS/A1300/01702A/007/2023/01193.

## Еріткішпен экстракциялау арқылы жоғары тазалықтағы празеодим мен неодимді алуудың технологиялық схемасын әзірлеу және модельдеу

<sup>1</sup> Zulkifli N., <sup>1\*</sup> Shoparwe N., <sup>1</sup> Yusoff A.H., <sup>2</sup>Abdullah A.Z., <sup>3</sup> Ahmad M. N.

<sup>1</sup> Малайзия университеті Келантан, Джели, Малайзия

<sup>2</sup> Малайзия ғылым университеті, Пенанг, Малайзия

<sup>3</sup> Малайзия Халықаралық Ислам Университеті, Куантан, Паханг, Малайзия

### ТҮЙІНДЕМЕ

Сирек жер элементтерін (СЖЭ) иондық адсорбцияланған саздардан (ИАЖ) тазартып, коммерциялық тазалыққа қол жеткізу үшін күрделі еріткіш экстракция (SX) жүйелері қажет. Бұл зерттеуде Малайзиядағы Джели кеңішінен алынған алдын ала өнделген REE хлоридін өңдеуге арналған төрт тізбекті қарсы ток SX ағындық сұлбасының дизайны мен валидациясы ұсынылады. Microsoft Excel бағдарламасындағы итеративті тұрақты күйдегі массалық балансты модельдеуді қолдана отырып жүргізілген зерттеу әрбір сирек кездесетін жер элементтері ағындарында 4N тазалық мақсатына (99,99%) жету үшін қажетті жұмыс параметрлерін анықтады. Әдістеме маңызды A/B бөлу кесінділерін дәл анықтауды және каскадтағы органикалық пен су (O/A) қатынастарын оңтайландыруды қамтыды. Нәтижелер сұлба шикізатты тиімді түрде фракциялайтынын көрсетеді, ол LREE/HREE (1-ші желі) көлемдік бөлүден бастап, празеодим (Pr) мен неодимді (Nd) кешенді бөлүмен аяқталады (4-ші желі). Модельдеу Pr/Nd бөлінүін негізгі технологиялық кедергі ретінде анықтады, ол 1,70 төмен бөлінүү коэффициентінен ( $\beta$ ) байланысты 62 тепе-тендік сатысын (NE) қажет етті. Ал қаралайым масса бөлінүлері тек 16 сатыны қажет етеді. Бұл нәтижелер теориялық минималды сатылы талаптарды ( $N_{min}$ ) растайды және әрбір пойыз үшін сатылы концентрацияның егжейтегейлі профилін ұсынады. Зерттеу нәтижесінде Pr/Nd қатынасы жалпы зауыт ауданын және оның күрделі қаржы сыйымдылығын анықтайды деген қорытынды жасалды. Әзірленген хаттама Малайзияның IAC ресурстарын коммерцияландырудың сенімді технологиялық жол картасын ұсынады, оңтайландырылған металлургиялық жобалау арқылы жоғары тазалықтағы СЖЭ алууды қамтамасыз етеді.

**Түйін сөздер:** СЖЭ бөлінүү, еріткішпен экстракциялау, P507, тепе-тендік қисығы, экстракция кезеңдері.

Мақала келді: 28 қараша 2025  
Саралтамадан етті: 30 қараша 2025  
Қабылданды: 20 қаңтар 2026

**Norazihan Zulkifli**

### Авторлар туралы ақпарат:

PhD докторант, Малайзия университеті Келантан, Джели 17600 Келантан, Малайзиядағы Биоинженерия және технология факультетінің Алтын, сирек жер және материалдар технокәсіпкерлік орталығы (GREAT). Email: norazihan.zulkifli@gmail.com; ORCID ID: <https://orcid.org/0009-0009-4772-0578>

**Noor Fazliani Shoparwe**

Қауымдастырылған профессор, Алтын, сирек жер және материалдар технологиялары орталығы (GREAT), Биоинженерия және технология факультеті, Малайзия университеті Келантан, Джели 17600 Келантан, Малайзия. Email: fazliana.s@umk.edu.my; ORCID ID: <https://orcid.org/0000-0002-4329-2459>

**Abdul hafidz Yusoff**

Қауымдастырылған профессор, Малайзия университеті Келантан, Джели 17600 Биоинженерия және технология факультетінің Алтын, сирек жер және материалдық технокәсіпкерлік орталығы (GREAT). Email: hafidz.y@umk.edu.my; ORCID ID: <https://orcid.org/0000-0003-0229-886X>

**Abdullah A.Z.**

Малайзия ғылым университеті, Химиялық инженерия мектебінің профессоры, 14300 Нибонг Тебал, Пулау Пинанг, Малайзия. Email: chzuhairi@usm.my

**Mohammad Norazmi Ahmad**

Тұрақты нанотехнология және есептей химиясы (SuNCoM) зерттеу тобының қауымдастырылған профессоры, Малайзия Халықаралық Ислам Университеті, 25200, Куантан, Паханг, Малайзия. Email: mnorazmi@iium.edu.my; ORCID ID: <https://orcid.org/0000-0001-5742-0346>

## Разработка и моделирование технологической схемы получения высокочистого празеодима и неодима методом экстракции растворителем

<sup>1</sup> Zulkifli N., <sup>1\*</sup> Shoparwe N., <sup>1</sup> Yusoff A.H., <sup>2</sup>Abdullah A.Z., <sup>3</sup> Ahmad M. N.

<sup>1</sup> Университет Малайзии Келантан, Джели, Келантан, Малайзия

<sup>2</sup> Университет науки Малайзии, Пенанг, Малайзия

<sup>3</sup> Международный исламский университет Малайзии, Куантан, Паханг, Малайзия

<p>Поступила: 28 ноября 2025 Рецензирование: 30 ноября 2025 Принята в печать: 20 января 2026</p>	<p><b>АННОТАЦИЯ</b> Очистка редкоземельных элементов (REE) для достижения коммерческой чистоты из ионно-адсорбированных глин (IAC) требует сложных систем экстракции растворителями (SX). В данном исследовании представлены проектирование и валидация четырёхпоеzdного противотокового SX расходного листа для переработки предварительно обработанного хлорида REE, полученного из месторождения Jeli в Малайзии. В исследовании, проведенном с использованием итеративного моделирования баланса массы в стационарном режиме в Microsoft Excel, определены рабочие параметры, необходимые для достижения целевого показателя чистоты 4N (99,99%) для каждого потока редкоземельных элементов. Методология включала точное определение критических разрезов между A/B и оптимизацию соотношения органического к водному (O/A) по всему каскаду. Результаты показывают, что схема эффективно фракционирует сырьё, начиная с массового разделения LREE/HREE (поезд 1) и заканчивая сложным разделением празеодима (Pr) и неодима (Nd) (Поезд 4). Симуляция определила разделение Pr/Nd как основное техническое узкое место, требующее 62 равновесных стадий (NE) из-за низкого коэффициента разделения (<math>\beta</math>) 1,70. В отличие от этого, более простые массовые сплиты требовали всего 16 этапов. Эти результаты подтверждают теоретические минимальные требования к этапам (<math>N_{min}</math>) и предоставляют подробный профиль концентрации по этапам для каждого поезда. Исследование пришло к выводу, что контур Pr/Nd определяет общую площадь завода и его капиталоёмкость. Разработанный протокол предлагает надёжный технический план коммерциализации ресурсов малайзийских IAC, обеспечивая высокочистое извлечение РЗЭ благодаря оптимизированному металлургическому проектированию.</p>
	<p><b>Ключевые слова:</b> разделение РЗЭ, экстракция растворителем, Р507, кривая равновесия, этапы экстракции.</p>
<p><b>Norazihan Zulkifli</b></p>	<p><b>Информация об авторах:</b> PhD докторант, Центр технопредпринимательства в области золота, редкоземельных элементов и материалов (GREAT), факультет биоинженерии и технологий, Университет Малайзии Келантан, Jeli 17600, Келантан, Малайзия. Email: norazihan.zulkifli@gmail.com; ORCID ID: <a href="https://orcid.org/0009-0009-4772-0578">https://orcid.org/0009-0009-4772-0578</a></p>
<p><b>Noor Fazliani Shoparwe</b></p>	<p>Ассоциированный профессор, Центр технопредпринимательства в области золота, редкоземельных элементов и материалов (GREAT), факультет биоинженерии и технологий, Университет Малайзии Келантан, Jeli 17600, Келантан, Малайзия. Email: fazliana.s@umk.edu.my; ORCID ID: <a href="https://orcid.org/0000-0002-4329-2459">https://orcid.org/0000-0002-4329-2459</a></p>
<p><b>Abdul hafidz Yusoff</b></p>	<p>Ассоциированный профессор, Центр технопредпринимательства в области золота, редкоземельных элементов и материалов (GREAT), факультет биоинженерии и технологий, Университет Малайзии Келантан, Jeli 17600, Келантан, Малайзия. Email: hafidz.y@umk.edu.my; ORCID ID: <a href="https://orcid.org/0000-0003-0229-886X">https://orcid.org/0000-0003-0229-886X</a></p>
<p><b>Abdullah A.Z.</b></p>	<p>Профессор Школы химической инженерии, инженерный кампус, Университет науки Малайзии, 14300 Небонг Тебал, Пулау Пинанг, Малайзия. Email: chzuhairi@usm.my</p>
<p><b>Mohammad Norazmi Ahmad</b></p>	<p>Ассоциированный профессор исследовательской группы по устойчивым нанотехнологиям и вычислительной химии (SuNCoM), кафедра химии, Международный исламский университет Малайзии, 25200 Куантан, Паханг, Малайзия. Email: mnorazmi@iium.edu.my; ORCID ID: <a href="https://orcid.org/0000-0001-5742-0346">https://orcid.org/0000-0001-5742-0346</a></p>

## References

- [1] Balaram V. Rare earth elements, resources, applications, extraction technologies, chemical characterization, and global trade – A comprehensive review. 2024. <https://doi.org/10.1016/B978-0-323-99762-1.00041-3>
- [2] Chang CS, Yusoff AH, Mohamed CAR, Liu SF, Shoparwe NF, Husain NA, & Azlan MN. Geochemistry of rare earth elements in Pahang river sediment, Malaysia. Kompleksnoe Ispolzovanie Mineralnogo Syra = Complex Use of Mineral Resources. 2024; 331(4):42–50. <https://doi.org/10.31643/2024/6445.37>
- [3] Salehi H, Maroufi S, Mofarah SS, Nekouei RK, & Sahajwalla V. Recovery of rare earth metals from Ni-MH batteries: A comprehensive review. Renewable and Sustainable Energy Reviews. 2023; 178:113248. <https://doi.org/10.1016/j.rser.2023.113248>
- [4] Balaram V. Sustainable recovery of rare earth elements by recycling of E-waste for a circular economy. 2024, 499–544. <https://doi.org/10.1016/B978-0-443-22069-2.00023-1>
- [5] Hua H, Yasuda K, Norikawa Y, & Nohira T. Highly efficient and precise rare-earth elements separation and recycling process in molten salt. Engineering. 2025; 45:165–173. <https://doi.org/10.1016/j.eng.2022.12.013>
- [6] Zhang Y, Gu F, Su Z, Liu S, Anderson C, & Jiang T. Hydrometallurgical recovery of rare earth elements from NdFeB permanent magnet scrap: a review. Metals. 2020; 10(6):841. <https://doi.org/10.3390/met10060841>
- [7] Hermassi M, Granados M, Valderrama C, Ayora C, & Cortina JL. Recovery of rare earth elements from acidic mine waters: An unknown secondary resource. The Science of the Total Environment. 2022; 810:152258. <https://doi.org/10.1016/j.scitotenv.2021.152258>
- [8] Wu M, Yu M, Cheng Q, Yuan Q, Mei G, Liang Q, & Wang L. Flotation recovery of Y2O3 from waste phosphors using ionic liquids as collectors. Chemical Physics Letters. 2023; 825:140608. <https://doi.org/10.1016/j.cplett.2023.140608>

[9] Gkika DA, Chalaris M, & Kyzas GZ. Review of methods for obtaining rare earth elements from recycling and their impact on the environment and human health. *Processes*. 2024; 12(6). <https://doi.org/10.3390/pr12061235>

[10] Shafiee NS, Achmad Bahar AM, & Ali Khan MM. Potential of rare earth elements (REEs) in Gua Musang granites, Gua Musang, Kelantan. *IOP Conference Series: Earth and Environmental Science*. 2020; 549(1):012027. <https://doi.org/10.1088/1755-1315/549/1/012027>

[11] Liu T, & Chen J. Extraction and separation of heavy rare earth elements: A review. *Separation and Purification Technology*. 2021; 276:119263. <https://doi.org/10.1016/j.seppur.2021.119263>

[12] Dewulf B, Riaño S, & Binnemans K. Separation of heavy rare-earth elements by non-aqueous solvent extraction: Flowsheet development and mixer-settler tests. *Separation and Purification Technology*. 2022; 290:120882. <https://doi.org/10.1016/j.seppur.2022.120882>

[13] Zulkifli N, Shoparwe NF, Yusof AH, Abdullah AZ, & Ahmad MN. From light to heavy: addressing gaps in rare earth element extraction at the lynas advanced materials plant. *Malaysian Journal of Bioengineering and Technology (MJBeT)*. 2024; 1(2):113–120. <https://doi.org/10.31643/2024/6445.32>

[14] Salehi H, Khani S, Adeli M, & Aboutalebi MR. Multistage hydrometallurgical process for enhanced recovery and individual separation of Nd and Pr from NdFeB magnet scrap. *Mineral Processing and Extractive Metallurgy*. 2024; 133(1-2):33-41. <https://doi.org/10.1177/25726641241233219>

[15] Ahmad I, Jamal MA, Iftikhar M, Ahmad A, Hussain S, Asghar H, Saeed M, Yousaf AB, Karri RR, Al-Kadhi NS, Ouladsmane M, Ghfar A, & Khan S. Lanthanum-Zinc Binary Oxide Nanocomposite with Promising Heterogeneous Catalysis Performance for the Active Conversion of 4-Nitrophenol into 4-Aminophenol. *Coatings*. 2021; 11(5). <https://doi.org/10.3390/coatings11050537>

[16] Azlina Y, Azlan MN, Halimah MK, Umar SA, El-Mallawany R, & Najmi G. Optical performance of neodymium nanoparticles doped tellurite glasses. *Physica B: Condensed Matter*. 2022; 577:411784. <https://doi.org/10.1016/j.physb.2019.411784>

[17] Nazrin SN, Halimah MK, Muhammad FD, Latif AA, Iskandar SM, & Asyikin AS. Experimental and theoretical models of elastic properties of erbium-doped zinc tellurite glass system for potential fiber optic application. *Materials Chemistry and Physics*. 2021; 259:123992. <https://doi.org/10.1016/j.matchemphys.2020.123992>

[18] Vani P, Vinitha G, Praveena R, Durairaj M, Sabari Girisun TC, & Manikandan N. Influence of holmium ions on the structural and optical properties of barium tellurite glasses. *Optical Materials*. 2023; 136:113438. <https://doi.org/10.1016/j.optmat.2023.113438>

[19] Yusof NN, Abd Azis MN, & Mohammad Yusoff N. Exploring the impact of plasmonic nanoparticles on photoluminescence of  $\text{Er}^{3+}$ -doped sodium zinc tellurite glass for solid-state laser applications. *Kompleksnoe Ispolzovanie Mineralnogo Syra = Complex Use of Mineral Resources*. 2024; 330(3):85-91. <https://doi.org/10.31643/2024/6445.32>

[20] Azlina Y, Azlan MN, Suriani AB, Shaari HR, Al-Hada NM, Umar SA, Kenzhaliyev BK, Zaid MHM, Hisam R, Iskandar SM, Yusof NN, & Yusoff AH. Incorporation of neodymium, holmium, erbium, and samarium (oxides) in zinc-borotellurite glass: Physical and optical comparative analysis. *Kompleksnoe Ispolzovanie Mineralnogo Syra = Complex Use of Mineral Resources*. 2025; 332(1):32–48. <https://doi.org/10.31643/2025/6445.03>

[21] Kumari H, Ansari GF, Mahajan SK, Rezaul K, & Bairagi S. Study of visible upconversion luminescence in  $\text{Er}^{3+}$  and  $\text{Er}^{3+}/\text{Yb}^{3+}$ -doped tungsten tellurite glasses. *Materials Today: Proceedings*. 2023. <https://doi.org/10.1016/j.matpr.2023.06.294>

[22] Wu Y, Niu C, Wang L, Yang M, & Zhang S. Structural, luminescence, and temperature sensing properties of the  $\text{Er}^{3+}$ -doped germanate-tellurite glass by excitation at different wavelengths. *Journal of Luminescence*. 2024; 266:120323. <https://doi.org/10.1016/j.jlumin.2023.120323>

[23] Zulkifli N, Shoparwe N, Yusof AH, Abdullah, AZ, & Ahmad MN. Ion exchange of lanthanum chloride and Lewatit Monoplus S 108 H resin. *Malaysian Journal of Bioengineering and Technology (MJBeT)*. 2025; 2(3):115-128. <https://doi.org/10.70464/mjbet.v2i3.1710>

[24] Talan D & Huang. QA review of environmental aspect of rare earth element extraction processes and solution purification techniques. *Minerals Engineering*. 2022; 179:107430. <https://doi.org/10.1016/j.mineng.2022.107430>

[25] Traore M, Gong A, Wang Y, Qiu L, Bai Y, Zhao W, Liu Y, Chen Y, Liu Y, Wu H, Li S, & You Y. Research progress of rare earth separation methods and technologies. *Journal of Rare Earths*. 2023; 41(2):182-189. <https://doi.org/10.1016/j.jre.2022.04.009>

[26] Pathapati SVSH, Free ML, Sarswat PK. A comparative study on recent developments for individual rare earth elements separation. *Processes*. 2023; 11(7). <https://doi.org/10.3390/pr11072070>

[27] Dorozhko, VA, & Afonin MA. Nonstationary separation of Nd and Pr by P507 extractant. *E3S Web of Conferences*. 2021; 266:02005. <https://doi.org/10.1051/e3sconf/202126602005>

[28] Pan J, Zhao X, Zhou C, Yang F, & Ji W. Study on solvent extraction of rare earth elements from leaching solution of coal fly ash by P204. *Minerals*. 2022; 12(12):1547. <https://doi.org/10.3390/min12121547>

[29] Afonin MA, Nechaev AV, Yakimenko IA, & Belova VV. Extraction of rare earth elements from chloride solutions using mixtures of P507 and Cyanex 272. *Compounds*. 2024; 4(1):172-181. <https://doi.org/10.3390/compounds4010008>

[30] Belova VV, Tsareva YuV, & Kostanyan AE. Extraction of rare-earth elements from chloride solutions in multicomponent systems using CYANEX 572. *Theoretical Foundations of Chemical Engineering*. 2022; 56(5):915-919. <https://doi.org/10.1134/S0040579522050025>

[31] Belova V, Petyaeva M, & Kostanyan A. Extraction of lanthanides from chloride solutions in hexane-isopropanol-water systems using Cyanex 572. *Theoretical Foundations of Chemical Engineering*. 2022; 56:595–599. <https://doi.org/10.1134/S0040579522040078>

[32] Dashti S, Shakibania S, Rashchi F, & Ghahreman A. Synergistic effects of Ionquest 801 and Cyanex 572 on the solvent extraction of rare earth elements (Pr, Nd, Sm, Eu, Tb, and Er) from a chloride medium. *Separation and Purification Technology*. 2021; 279:119797. <https://doi.org/10.1016/j.seppur.2021.119797>

[33] Salehi H, Maroufi S, Khayyam Nekouei R & Sahajwalla V. Solvent extraction systems for selective isolation of light rare earth elements with high selectivity for Sm and La. *Rare Metals*. 2025; 44(3):2071–2084. <https://doi.org/10.1007/s12598-024-03019-7>

[34] Srivastava V, Werner J, & Honaker R. Design of multi-stage solvent extraction process for separation of rare earth elements. *Mining*. 2023; 3(3):552–578. <https://doi.org/10.3390/mining3030031>

[35] Krishnamurthy N, & Gupta CK. Extractive metallurgy of rare earths (0 ed.). CRC Press. 2015. <https://doi.org/10.1201/b19055>

[36] Merroune A, Ait Brahim J, Berrada M, Essakhraoui M, Achiou B, Mazouz H, & Beniazz R. A comprehensive review on solvent extraction technologies of rare earth elements from different acidic media: Current challenges and future perspectives. *Journal of Industrial and Engineering Chemistry*. 2024; 139:1–17. <https://doi.org/10.1016/j.jiec.2024.04.042>

[37] Turgeon K, Boulanger JF, Bazin, C Turgeon K, Boulanger JF, & Bazin C. Simulation of solvent extraction circuits for the separation of rare earth elements. *Minerals*. 2023; 13(6). <https://doi.org/10.3390/min13060714>